NUMERICAL THERMAL MODELING OF THE WIPP IN SITU ROOM A1 SIMULATED DHLW EXPERIMENTS*

Richardo Beraun and Martin A. Molecke
Sandia National Laboratories
Albuquerque, NM 87185

ABSTRACT

The intent of this paper is to present the results of transient thermal analyses performed to determine temperatures in the near- and far-field, in the vicinity of a defense high-level waste container and an emplacement drift. Three different drift/canister configurations were modeled; one containing nitrogen gas, another crushed salt, and the last bentonite/sand as the backfill material between the container and the borehole wall. The test containers are a non-reference overpack design, consisting of a 2.5 cm thick mild steel container either with or without a thin overwrap of TiCode-12. The thermal conductivity of the salt formation was assumed to be temperature dependent while both the density and specific heat were assumed to be constant. The analyses were undertaken using a four node, bilinear, quadrilateral finite element nonlinear heat transfer program, COYOTE, and a finite difference thermal analyzer code, SINDA. Results presented include typical temporal and spatial distributions of temperature. The near-field temperature results obtained from the numerical modeling compare well with measured experimental data.

INTRODUCTION

The need for permanent long term storage of radioactive waste products has led to a number of proposals involving burial of the waste in various geologically stable regions of the earth. The Waste Isolation Pilot Plant (WIPP) is the site for research and development including the borehole emplacement of defense high-level waste (DHLW) packages. The WIPP is authorized to demonstrate the safe disposal of radioactive wastes resulting from the defense activities and programs of the United States. Several series of waste package performance technology experiments for simulated DHLW packages have been emplaced and put into active operation at the WIPP facility (1). These experiments involve 18 full-size nonradioactive DHLW packages emplaced in heavily instrumented vertical boreholes in the salt drift floor. Planned test duration is 3 to 7 years.

The test DHLW packages (i.e., containers, backfills and waste form) are located in vertical boreholes in the rock salt floor of two test rooms in the WIPP. The test rooms are located at a depth of about 650 m below the surface. Six simulated DHLW packages are located in WIPP Room A1 under near-reference repository thermal conditions. Each of these containers incorporates an internal electric heater with an average thermal output of 470 watts. A major purpose of these waste package performance (WPP) experiments (2) is to evaluate the in situ materials performance (i.e., degradation or alteration) of various waste package components: metal containers and overpacks, backfill materials, nonradioactive DHLW glass, and installed instrumentation. To aid in accomplishing the experimental objectives, extensive numerical thermal modeling has been conducted to predict the near-field and far-field thermal behavior and to compare these with the actual measured thermal distributions. These thermal modeling efforts are also an important element of the waste package performance assessment. The determination of temperature histories of the waste package and surrounding host rock salt is essential for the testing program to determine the geochemical conditions, permeability, and other properties of backfill (sometimes referred to as "packing") materials.

ANALYSIS OBJECTIVE

The objective of these analyses is to define and develop thermal models that would help in predicting the thermal environment that will exist around defense high level waste (DHLW) containers and in the surrounding rock salt formation. The information obtained from these thermal analyses is essential in helping define a number of parameters when performing WIPP waste package performance assessments. Some of these parameters include permeability and thermal conductivity values for backfill materials. These parameters are necessary to further determine the geochemical conditions. These thermal analyses are also essential in the determination of thermal stresses and the hydraulic behavior associated with the host rock salt.

GEOMETRY AND FACILITY DESCRIPTION

The Waste Package Performance Technology Experiments for simulated (nonradioactive) defense high level waste (DHLW) (1,2) are a series of in situ experiments that are intended to evaluate the moderate-to-long-term performance of DHLW package barrier materials (2). Barrier material performance is being evaluated using data obtained from short term (3 to 7 years) tests and overtests, under both expected near-reference and severe-overtest salt repository environmental conditions.

*This work performed by Sandia National Laboratories, supported by the U.S. Department of Energy under Contract DE-AC04-76DP00789.

Physical Location

The WIPP test rooms are approximately 650 m below ground level. A plan view of the general underground layout of the WIPP facility is illustrated in Fig. 1. The in situ test geometry for near-reference simulated DHLW experiments consists of three parallel rooms, each approximately 5.5 m square in cross section by 93.3 m long, spaced 23.5 m center-to-center. Room A1 waste packages are emplaced into vertical boreholes in the salt floor in a single-row configuration, 1.9 m apart. Each borehole is either 0.76 m or 0.91 m (30 and 36 inches) in diameter and 5.5 m deep. The vertical location of these experiments is depicted in Fig. 2, which is essentially an elevation view that shows major stratigraphic features. Fig. 3 shows a typical cross section of a simulated DHLW emplacent in Room A1. Also depicted in this figure is, the waste container and borehole arrangement indicating the two different borehole diameters.

Waste Package Description

All six waste containers (canisters) in Room A1 are, basically, a Sandia developmental canister-overpack design for DHLW. They are fabricated from schedule 60 mild steel pipe, nominally 3.0 m tall, 0.61 m in diameter, and with a 2.5 cm-thick wall (2). They have flat top and bottom heads and a top handling pintle identical to that used on other "reference" design containers (1,2). Some of these test canister-overpacks have a 2.2 mm thick TiCode-12 overlay wrapped and welded around the mild steel, as well as TiCode-12 pintles. All Room A1 test containers have internal electric heaters with an average power output of 470 watts each. Waste packages are emplaced into vertical boreholes in the salt floor in a single-row configuration, 1.9 m apart. Each borehole is either 0.76 m or 0.91 m in diameter and 5.5 m deep. Additional details, operational discussions, and observations of all types of test DHLW containers are described elsewhere (1,2).

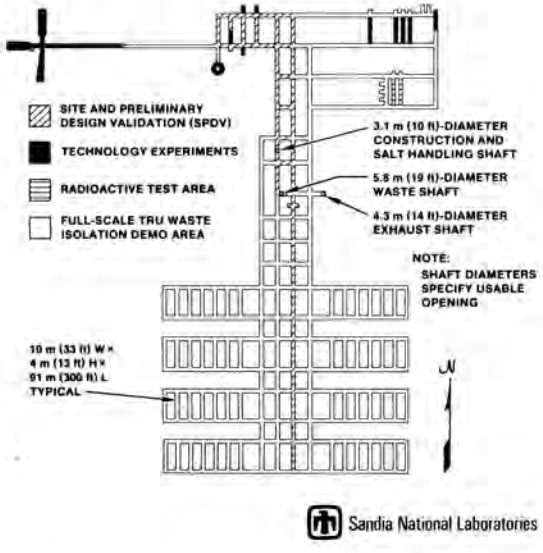

Fig. 1. General Underground Layout of the WIPP Facility.

MODELING EFFORTS

Problem Definition

The construction of the models for the required calculations involved several important features, some of these being the discretization of the domain to geometrically represent the physical situations, the establishment of the proper initial and boundary conditions, the definition of the domain within which to perform the calculations, and the identification of the different materials in the stratigraphy involved and their constitutive properties. Geomechanical data for thermal analyses were obtained from several sources. The emplacement drift geometry was obtained mostly from the Test Plan: "Waste package Per formance Technology Experiments for Simulated DHLW," prepared by M. A. Molecke (2). The assumed stratigraphy and rock properties were obtained from a report entitled "Reference Stratigraphy and Rock Properties for the WIPP project," prepared by R. D. Krieg (3).

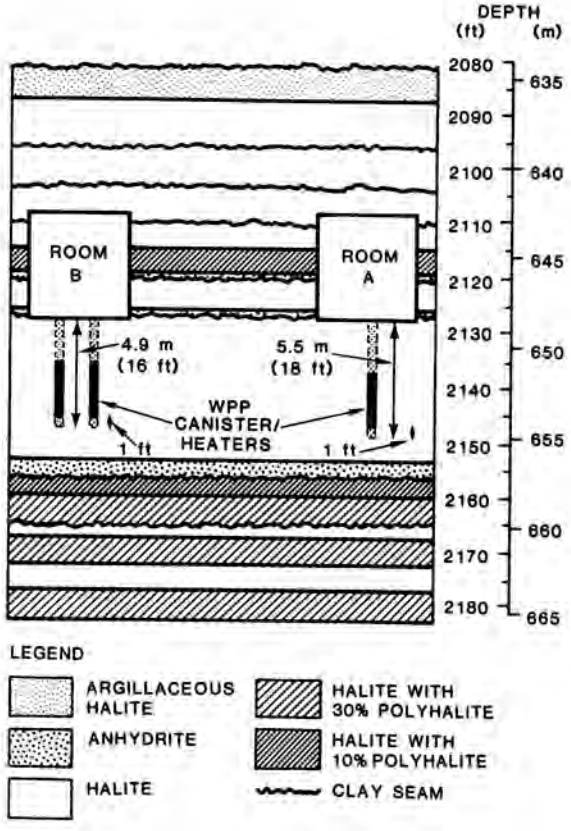

Fig. 2. Vertical Location of Waste Package Performance Experiments.

Essentially, two backfill materials were considered in these analyses. These materials were crushed salt and a blend of bentonite and silica sand, in the ratio of 70 percent to 30 percent by weight, respectively. In addition a third case was evaluated, with nitrogen gas filling an open annulus between the container and the borehole walls.

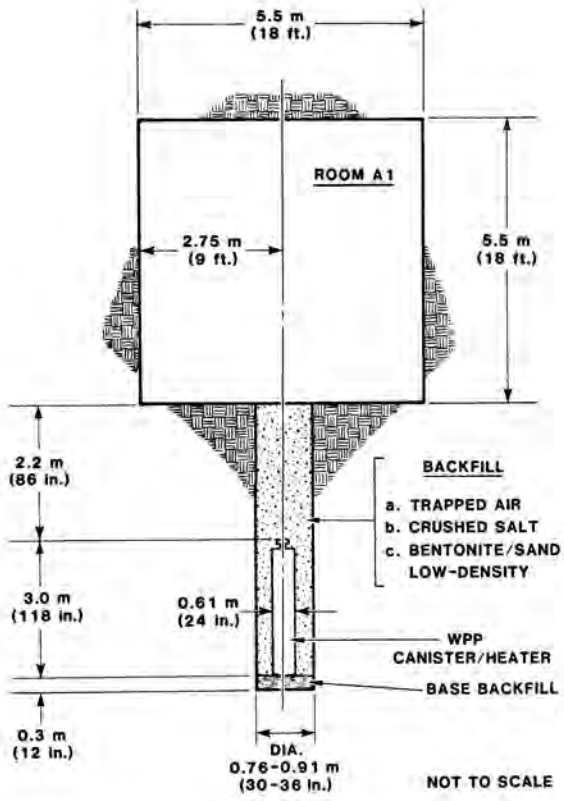

Fig. 3. Cross Section of a Simulated DHLW Emplacement in Room A1.

Assumptions

The models constructed for these thermal studies are based on several assumptions. The most important ones are as follows.

- All waste packages are simultaneously emplaced in the repository. With this assumption, the geometrical symmetry consideration can be employed. A single slab, symmetrically cut through a waste package, represents the typical waste package and its environment. (For the simulated DHLW experiments (2) being modeled, all of the electric heaters were turned on simultaneously.)
- All components of the waste package (i.e., waste form, container, backfill material) are made of isotropic and homogeneous materials.
- The heat of vaporization and condensation of groundwater in the formation and the convective transport of heat are not considered.
- The drift is unventilated and the radiative heat transfer taking place is appoximated by ascribing equivalent conductivity properties to air, as derived from an effective radiation conductivity analysis in the drift (described in a later subsection).
- For a given stratigraphy of the rock mass, it is assumed that nonlinear effects, including pore water migration, can be ignored. In practice, nonlinear effects and the specific configuration of the container, container borehole, and the backfill material thermal behavior could strongly influence very-near-field conditions.

THERMAL ANALYSIS

Thermal Properties

The cross section of the region where the waste container tests are being performed consists of several layers of nonsimilar materials. These strata vary in thickness from 0.08 m to 19.39 meters. Their properties and spatial location are given in Table I and in Ref. 3 respectively. Many of the regions are located at a distance greater than 10 m from the container and drift. It was assumed that average material properties could be used to combine actual strata. Material density, specific heat and the conductivity exponent, γ, were geometrically averaged. The thermal conductivities were averaged using a series model,

$$\sum \frac{L}{k} = \frac{L_1}{k} + \frac{L_2}{k} + \ldots \frac{L_i}{k} \qquad (1)$$

where L_i is the thickness of the i^{th} strata. The thermal conductivity of the materials in the stratigraphy was assumed to vary with temperature according to

$$k(T) = k_{300}\left(\frac{300}{T}\right)^{\gamma} \qquad (2)$$

where k is the material's thermal conductivity at a given temperature T, k_{300} is its conductivity value at some reference point (300 K for this case, the ambient underground temperature at the WIPP facility), and γ is the conductivity exponent (4).

Thermal conductivity values of the backfill materials used in these calculations were derived in previous thermal analyses (5) by fitting parametric calculations to measured in situ temperature (as measured with installed thermocouples) versus time data. These thermal conductivity values are tabulated in Table II. Additional and more detailed information on these values are found in a previous report (5).

TABLE I

Material Thermal Properties

Material	Density ρ kg/m^3	Specific Heat C_p J/kg-K	Thermal Conductivity k w/m-K	Parameter γ
Arg. Salt	2167	860	4.0	1.14
Halite	2300	860	5.0	1.14
Anhyd. MB136	2170	860	4.14	1.14
Anhyd. MB139	2167	860	4.5	1.14
Anhydrite	2200	860	4.9	1.14
Polyhalite	2167	860	3.6	1.14
Air	1.0	1000	46.0†	0.0

†Effective Rad. Cond. value see Fig. 5.

Tools for Numerical Modeling

The SINDA (6) and the COYOTE (7) heat transfer codes were chosen as tools to model the problem. Because of complexity due to the model geometry and the transient nature of the problem, model development and results from both codes were checked against each

TABLE II

Thermophysical Properties of Backfill Materials

Backfill Material	Density ρ kg/m^3	Specific Heat C_p J/kg-K	Thermal Conductivity k w/m-K
Crushed Salt	1290	860	1.12
Bentonite/sand	1260	860	0.28†
Nitrogen Gas	0.998	1042	0.451‡

†0.43 for temperatures above 420° K

‡Effective Rad. Cond. value see Fig. 4.

other and compared with some available test results to ensure appropriate model thermal responses. SINDA is a versatile code based on the lumped-heat-capacity approach for solving primarily conduction-dominated problems. This tool for thermal analysis contains numerous subroutines for handling interrelated complex phenomena. The COYOTE code is a finite element nonlinear heat transfer computer program. For the case where the SINDA code was utilized, the transient thermal analysis was performed using the CNBACK subroutine, which is essentially an implicit backward-differencing technique. In the case where COYOTE was used as the tool for conducting the transient analysis, the Crank-Nicolson method for time integration, and a four node, bilinear, quadrilateral element type was used.

The generation of the nodal network of this system as used by SINDA was facilitated by the HEATMESH-71 (9) computer code. HEATMESH is a computer code for generating the geometric data required for studies of heat transfer in axisymmetric structures and consists of two distinct phases. The first subdivides the part into a network of nodes and evaluates the geometrical properties of each node. The second determines adjacent nodes and specifies their interconnection for SINDA. The finite element mesh used in conjunction with COYOTE was generated using mesh generators that are an integral part of the code. A very fine grid size (relative to overall size) was used within the waste package to provide realistic temperature predictions. As the distance from the waste package increases, the grid sizes gradually increased. This approach is based on the fact that the thermal gradient diminishes as the distance from the heat source increases. By symmetry, only half of the drift configuration was needed to calculate the required thermal response.

These computer thermal computations were done on a CRAY computer system, using the SINDA code mostly for the near-field calculations, and the COYOTE code for both the near- and far-field computations. The analyses were nonlinear and transient, and the Crank-Nicolson method was used for time integration. The computations required approximately 25 seconds to calculate 20 time steps for the 0.31 years (112 days) simulation, with SINDA, and 35 seconds to calculate 30 time steps for the 1 year (364 days) simulation, with COYOTE. Although, the models have the capability to exceed these time frames, analyses were conducted for these simulation time periods only for the purpose of comparing results with available measured test data.

Thermal Radiation Analysis

In all cases, the computer codes used in this study considered only conductive heat transfer. For situations where thermal radiation needed to be accounted for, it was treated indirectly by deriving an effective radiation conductivity k_{reff} (8,10). For the case where thermal radiation in the gap between the container and the borehole (filled with nitrogen) needs to be accounted for, the radiation heat transfer for infinitely long concentric cylinders was equated to conduction in the radial direction, to obtain a relationship for k_{reff} as a function of a single temperature. The effective radiation conductivity approach was also used for radiation heat transfer across the drift (11,12). For this situation one needs to set the radiation heat transfer between infinite parallel plates equal to conductive heat transfer taking place between these plates. The details of the algorithm involved in the development of the applicable relationships can be found in Ref. 8. Fig. 4 shows the effective radiation conductivity for the annular space between the container and the borehole wall. Fig. 5 depicts the effective radiation conductivity for the drift.

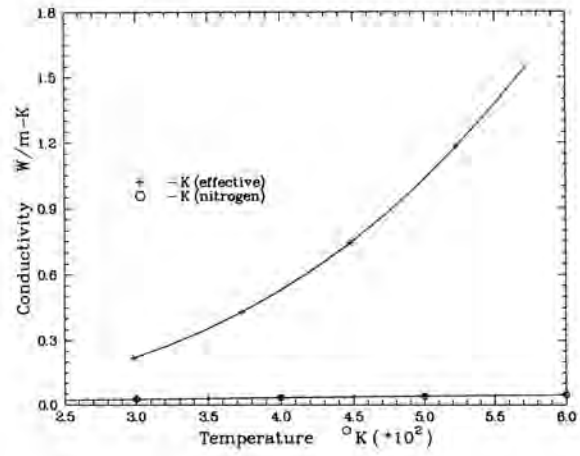

Fig. 4. Effective Radiation Conductivity for the Annular Space Between the Container and the Borehole Wall.

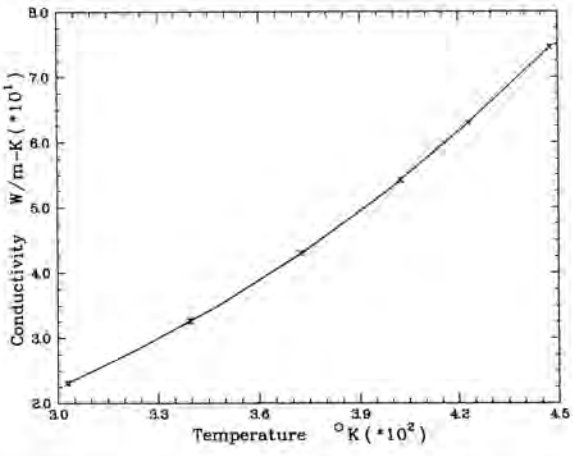

Fig. 5. Effective Radiation Conductivity for the Drift.

Heat Sources, Initial and Boundary Conditions

There are several types of decay laws that could realistically represent the waste heat output in

these type of problems. For purposes of simplicity, the heat source output in these thermal analyses is assumed to follow an exponential decay of the form (14)

$$P = P_0 \exp^{-\lambda t} \qquad (3)$$

where Po is the initial power density at the time of disposal and λ is the decay constant.

Throughout the modeling, the system was assumed to start at a uniform temperature of 300 K, the ambient temperature in the underground WIPP facility. Because of the large geometrical dimensions associated with the model, the specification of adiabatic boundary conditions to all exterior element boundaries is a very good approximation of the real situation. Calculations to check on the validity of these conditions were made by other analysts in similar types of problems (14,15). This comparison was made by performing the same computer runs using isothermal boundaries. The effect of changing these boundary conditions was insignificant causing less than a 1 K temperature change in the near region.

DISCUSSION OF RESULTS

Results from this study are summarized in Figs. 7 through 12 and Table III. The curves depicted in these figures are typical temporal and spatial distributions of temperature for each case. The results tabulated in Table III are maximum calculated temperatures for three locations in the near-field; namely, at the container inner and outer wall interface, the backfill midpoint and the borehole wall surface. Although, the model is set up to handle varying thermal heat sources, it is not equipped to handle either power fluctuations or power losses as they were observed during the heated phase of these experiments. Since the times for which the calculations are carried out are short in terms of power decay effects, the exponential decay equation above mentioned is still applicable. The results presented in this report are for Room A1 DHLW test packages where each of the containers incorporates an internal electric heater with a nominal thermal output ranging between 470 and 500 watts. The power level throughout each calculation was almost unchanged from its initial state. In this thermal study, a combination of six waste container systems and three backfill materials were investigated. The results presented in this report will be divided into two sections. The first section will consist of temperature responses in the near-field and the second section will consist of results in the far-field. Because of the vast amount of computational plots representing both the near and the far-field results of all six container systems, only those for the mild steel container with nitrogen gas backfill system are presented in this section. Comparisons with a similar system (with TiCode-12 overwrap) in the near-field are made. A complete compilation of all the results can be found in Ref. 8.

Near-Field Results

The near-field region results for the system above mentioned are given in Figs. 7 through 9 as a series of time-history plots of particular model points that are identified in Fig. 6 (point A is on the inner wall surface of the test container, point B is on the outer wall surface of the test container and point C is on the wall of the salt borehole, all points being at the container midheight level). Figs. 7 and 8 are temperature profiles for the container mid-height inner wall surface and the borehole mid-height wall surface, corresponding to the mild steel container (WA1) and to the mild steel container with TiCode-12 overwrap and pintle (WA2), respectively. Nitrogen gas fills the space between the container and the borehole wall. Although the same power level was utilized in both container models, it was found that their temperature responses are different. The difference in the thermal responses is attributed to different overall thermal properties associated with each waste container system. The effect of the extra insulating layer provided by the TiCode-12 overwrap is shown in Fig. 9. This figure depicts the temperature history at the container mid-height surface wall for both the mild steel container and the mild steel/TiCode-12 overwrap container. It shows, in essence, that the TiCode-12 overwrap acts as an insulator, delaying the heat transfer to the surrounding nitrogen gas and allowing the wall surface to reach higher temperatures than in the case without the TiCode-12 overwrap. The temperature rise-times and temperature profiles predicted by the numerical model are in good agreement with the experimental results for both container systems. Temperatures of approximately 333 K (60°C) for the container mid-height surface, and, 322 K (49°C) for the borehole mid-height wall surface are attained for container WA1, at the end of 112 days after heater turn on. The corresponding temperatures for the same locations of container system WA2 are 342 K (69°C) and 325 K (52 °C).

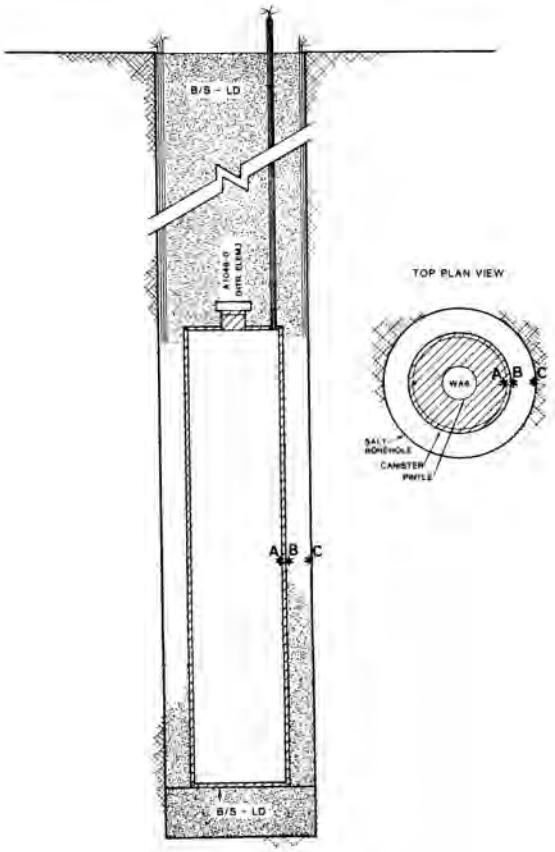

Fig. 6. Locations of Points for Time-History Plots.

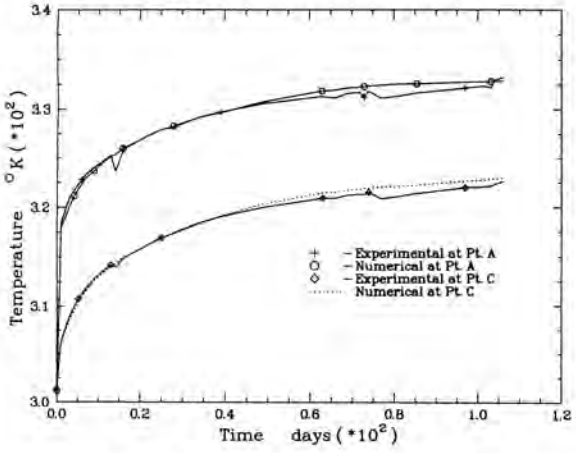

Fig. 7. Near-Field Temp. Profiles for Container System WA1 (Mild Steel Test Container, Nitrogen Backfill)

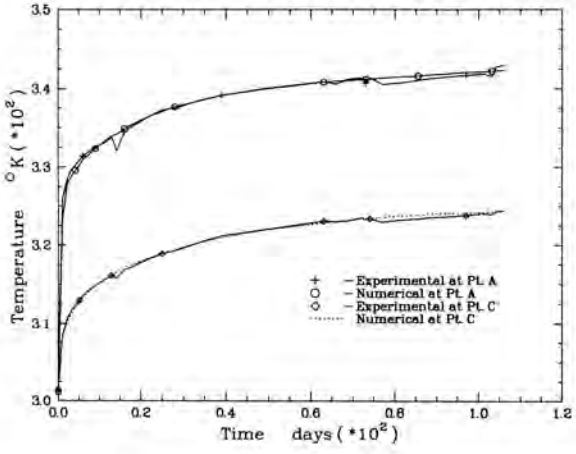

Fig. 8. Near-Field Temp. Profiles for Container System WA2 (Mild Steel Container with TiCode-12 Overwrap, Nitrogen Backfill)

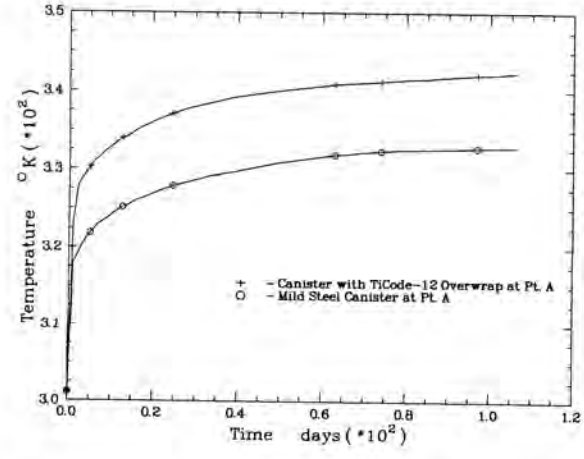

Fig. 9. Container Mid-Height Surface Temperature History Summarizing the Effect of the TiCode-12 Overwrap for Systems WA1 and WA2

TABLE III

Maximum Calculated Temperatures
1 Year After Heater Turn On

Container System	Backfill Material	Container Interface °K	Backfill Midpoint °K	Rock Salt Interface °K
WA1	Nitrogen gas	333†	-	322†
WA2	Nitrogen gas	342†	-	325†
WA3	Bentonite/Sand	336	-	321†
WA4	Crushed Salt	324	-	318†
WA5	Crushed Salt	329	322†	319†
WA6	Bentonite/Sand	354	329†	317†

†Temperatures are still increasing

Far-Field Results

The far-field in this analysis comprises the region beyond the borehole surface wall (into the formation). The temperature contours were observed to be of similar patterns for all container systems. The far-field results for the system described above are summarized in Figs. 10 through 12. Fig. 10 depicts the temperature response vertically along the configuration for container system, at selected times after heater turn on. The horizontal coordinate in this figure represent the vertical distance along the configuration where the 0.0 coordinate of this scale corresponds to a point 52.87 m below Clay G, the reference zero described in the latest update to the reference stratigraphy (4). Maximum temperatures are recorded, as expected, at the container midplane located about 3.128 m below the drift floor, corresponding approximately to a distance of 49.0 m on the horizontal scale in Fig 10. The effect of the drift on the temperature gradient is indicated by the change of the slope of the temperature curves at approximately 53.0 m on the horizontal scale of Fig. 10.

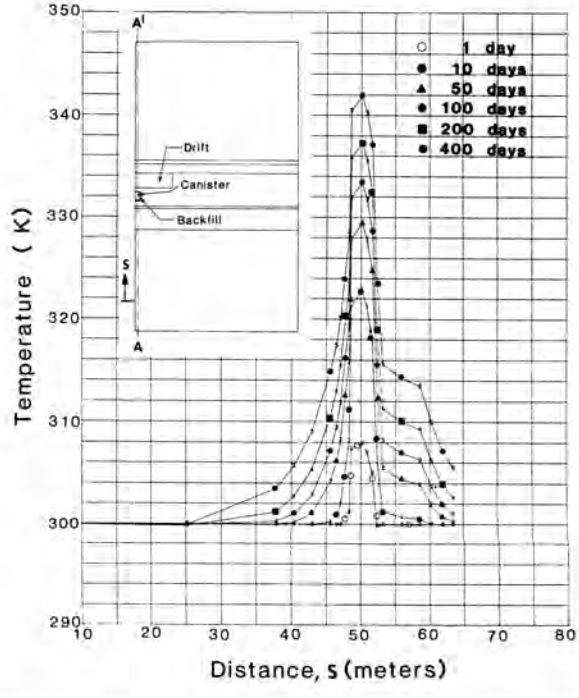

Fig. 10. Temperature Profiles Along Vertical Line A-A' for Container WA1

Fig. 11 shows temperature profiles along a horizontal plane through the configuration at the container mid-height level into the formation. The abscissa in this figure represent the horizontal distance through the container midplane where the 0.0 coordinate of this scale corresponds to the container center point at mid-height level. As expected, the highest temperature is recorded at the center of the container and diminishes into the formation. This curve corresponds to 6 different time intervals, namely at the end of the 1st, 10th, 50th, 100th, 200th, and the 400th day. The locations of the vertical and horizontal distance represented by the abscissa in Figs. 10 and 11 are indicated in the inset sketch of the region being modeled.

Fig. 12 illustrates typical spatial temperature distributions for a region around the container configuration. The contours of temperature rise depicted in these curves, range from 300 K (27 C) to 360 K (87 C). They represent temperature increments of 5 K. These contour plots correspond to six time intervals indicated in the figures. The same pattern of temperature contours was found for the other container systems where various temperature ranges were observed (8).

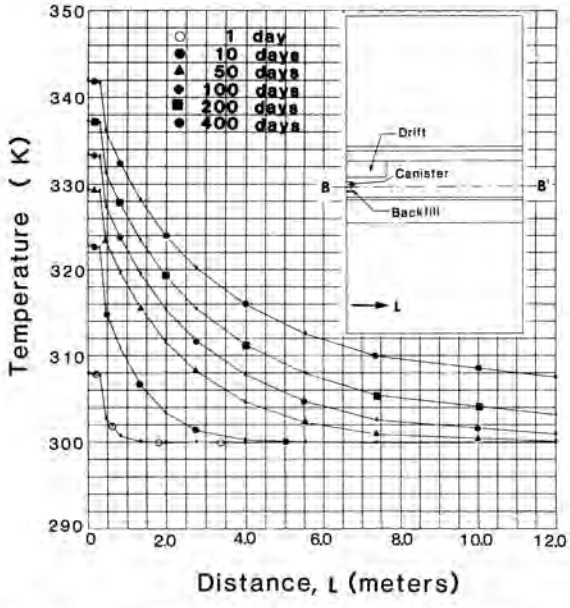

Fig. 11. Temperature Profiles Along Horizontal Line B-B' for Container WA1

CONCLUSIONS

To aid in accomplishing the experimental objectives (2), extensive thermal analyses were conducted to predict the near-field and the far-field thermal behavior for a simulated defense high-level waste package test system. The determination of temperature histories of the waste package systems and surrounding host rock salt is essential for the test program to help determine and interpret the geo-chemical conditions, permeability, and thermal conductivities of backfill materials (5). These histories are needed also to determine thermal stresses and the hydraulic behavior of host rock salt. The analytical results presented in this report appear to agree well with experimentally measured data (5) for the types of backfill materials utilized. However,

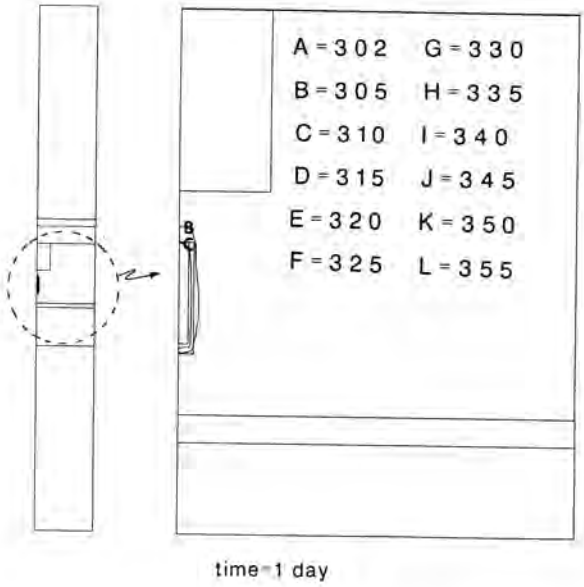

Fig. 12. Contours of Temperature Rise (°K) for Container WA1

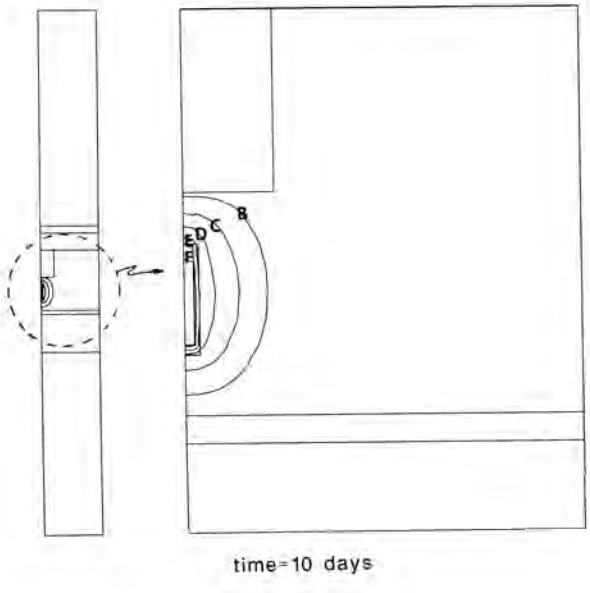

Fig. 12. Contours of Temperature Rise (°K) for Container WA1 (cont.)

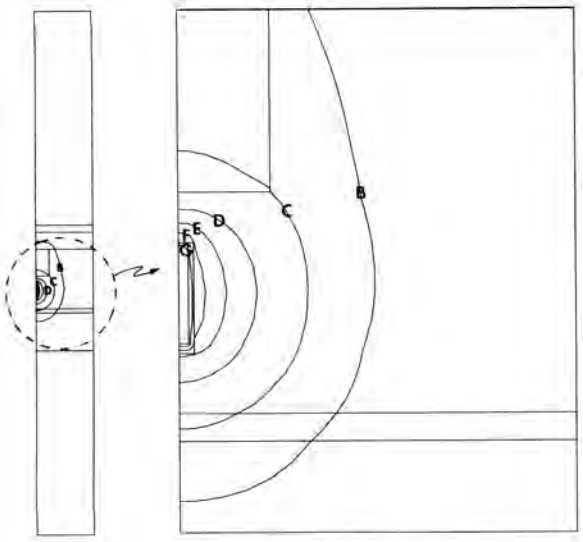

time=50 days

Fig. 12. Contours of Temperature Rise (°K) for Container WA1 (cont.)

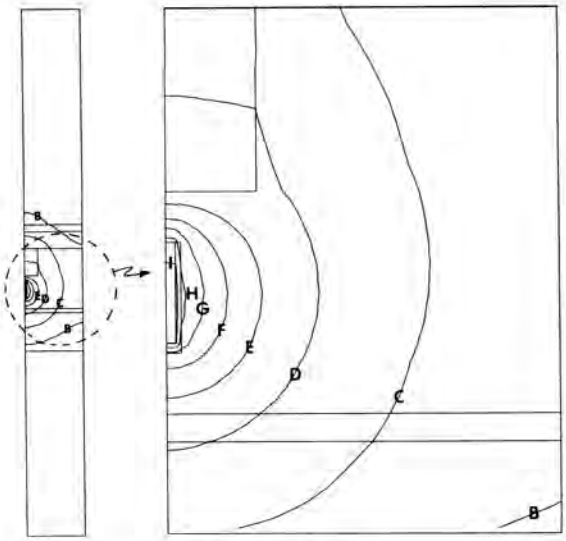

time=190 days

Fig. 12. Contours of Temperature Rise (°K) for Container WA1 (cont.)

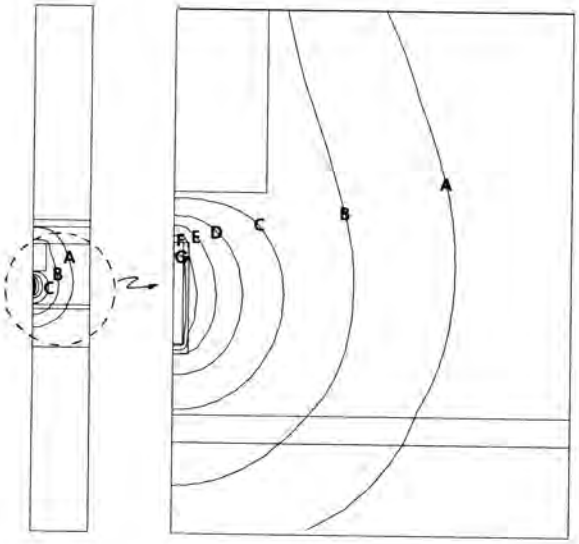

time=100 days

Fig. 12. Contours of Temperature Rise (°K) for Container WA1 (cont.)

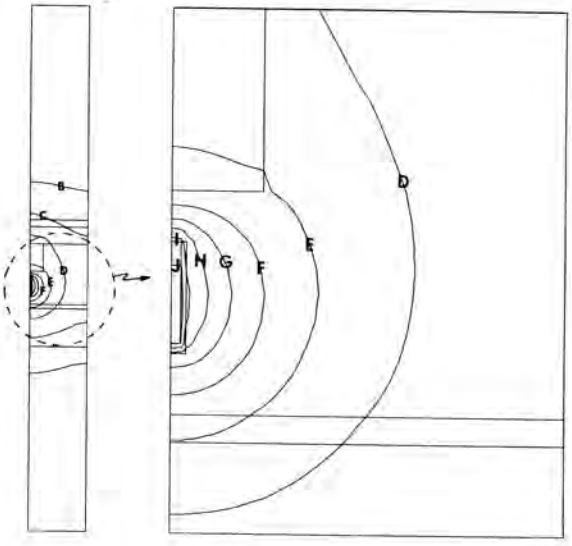

time=365 days

Fig. 12. Contours of Temperature Rise (°K) for Container WA1 (cont.)

appreciable discrepancies are noticeable between the measured and the calculated temperature responses during the first days after heater turn on, specifically for the container systems where the backfill materials were other than gas. These discrepancies are believed to be due to the presence of air and moisture initially residing in the backfill near the waste-container/ backfill surface interface. This effectively results in smaller thermal conductivity values, making the interface region act as an insulator. Before this interface region becomes thermally stable, the container surface temperature rises rapidly. Once the backfill material in the interface region attains a quasi-stable condition, then heat is conducted more efficiently through the region. Modeling efforts focusing on the first several days after heater turn-on will be the topic of a subsequent report.

It is anticipated that these methods can be applied in other calculations of similar models involving different backfill materials and different waste container emplacement geometries. The calculational methods utilized in this calculations as described in Ref. 8 will also be used specifically (in a subsequent report) to determine the in situ thermal conductivities of waste package backfill materials as a function of the following variables: time, material composition, density, temperature, moisture content, and position within the waste package emplacement.

REFERENCES

1. Molecke, M. A., "WIPP Waste Package Performance Testing on Simulated DHLW: Early Data," SAND85-0559C, published in High-Level Nuclear Waste Disposal, edited by H. C. Burkholder, Batelle Press, Columbus, OH (1986).

2. Molecke, M. A., "TEST PLAN: Waste Package Performance Technology Experiments for Simulated DHLW," Sandia National Laboratories (June 1984).

3. Krieg, R. D., "Reference Stratigraphy and Rock Properties for the Waste Isolation Pilot Plant (WIPP) Project," SAND83-1908, Sandia National Laboratories (1984).

4. Eaton, R. R., "Three-Dimensional Thermal Analysis for the WIPP In Situ Test Room A2 Heater Configuration," SAND84-2220, Sandia National Laboratories (1984).

5. Molecke, M. A. and Beraun, R., "WIPP Simulated DHLW Tests: Status and Initial In Situ Backfill Thermal Conductivities," SAND86-0489C, Sandia National Laboratories (1986).

6. TRW, Systems Group, Systems Improved Numerical Differencing Analyzer (SINDA), 14690-HY001-RO-00, 1971.

7. Gartling, D. K., "COYOTE--A Finite Element Program for Nonlinear Problems," SAND77-1332, Sandia National Laboratories (1978).

8. Beraun, R. and Molecke, M. A., "Thermal Analysis of the WIPP In Situ Room A1 DHLW Package Experiments," SAND86-0681, Sandia National Laboratories (1987).

9. Gabrielson, V. K., HEATMESH-71: A Computer Code for Generating Geometrical Data Required for Studies of Heat Transfer in Axisymmetric Structures, SCL-DR-72004, 1972.

10. Carnahan, B., Luther, H. A., and Wilkes, J. O., Applied Numerical Methods, John Wiley & Sons, Inc., New York, 1969.

11. Bulmer, B. M., "Pretest Thermal Analysis of the Tuff Water Migration/In Situ Heater Experiment," SAND79-1278, Sandia National Laboratories (1980).

12. Rohsenow, W. M. and Hartnett, J. P., Handbook of Heat Transfer, McGraw-Hill Book Company, NY (1973).

13. Siegel, R. and Howell, J. R., Thermal Radiation Heat Transfer, McGraw-Hill Book Company, NY (1972).

14. Mufti, I. R., "Geothermal Aspects of Radioactive Waste Disposal into the Subsurface," J.Geophysics Res., Vol. 26, No. 35, December 1971.

15. Eaton, R. R., Two-Dimensional Thermal Analysis of the In Situ WIPP Heater Experiment A2, Memo to Distribution, Sandia National Laboratories, February 25, 1985.